Reaction Pathways in Solid-State Processes. 1. Carbon-13 NMR and X-ray Crystallography of Fluorobullvalene

K. Müller,[†] H. Zimmermann,[‡] C. Krieger,[‡] R. Poupko,[§] and Z. Luz*[,§]

Contribution from the Institut für Physikalische Chemie, Universität Stuttgart, D-70569 Stuttgart, Germany, Max-Planck-Institut für Medizinische Forschung, AG Molekülkristalle, D-69120 Heidelberg, Germany, and The Weizmann Institute of Science, 76100 Rehovot, Israel

Received November 28, 1995. Revised Manuscript Received May 14, 1996[⊗]

Abstract: Carbon-13 MAS−NMR and X-ray diffraction experiments on solid fluorobullvalene are reported. The compound crystallizes in the orthorhombic space group *Pnam* with four symmetry related molecules per unit cell. The crystal consists entirely of isomer 4 (in which the fluorine is bound to the bridgehead carbon). Temperature dependent 1D and 2D NMR exchange experiments reveal the occurrence of two independent dynamic processes, both preserving the crystal order, but on a completely different time scale. The faster of the two processes involves 3-fold jumps about the molecular (pseudo) C_3 symmetry axis. Line shape analysis of dynamic 1D MAS spectra yields an Arrhenius rate equation with a pre-exponential factor, $A_J = 6.0 \times 10^{17}$ s^{-1}, and an activation energy, $E_J = 21.7$ kcal mol^{-1}. The mechanism of this process was confirmed by a rotor synchronized 2D exchange experiment performed with a mixing time of 20 ms. This spectrum exhibits auto cross peaks between spinning side bands of the same types of carbons, but no hetero cross peaks linking different types of carbons. Two-dimensional exchange spectra recorded on a much longer time scale (of the order of seconds) exhibit, in addition, hetero cross peaks between the main and spinning side bands of different types of carbons. These cross peaks can only result from Cope rearrangement involving other isomers of fluorobullvalene as intermediates. It is argued that the dominant mechanism of this process involves the sequence: isomer 4 → isomer 1 → isomer 3 → isomer 1 → isomer 4, where isomers 1 and 3 serve as transient intermediates. Magnetization transfer experiments provide the following estimates for the kinetic parameters of this process, $A_C = 4.6 \times 10^9$ s^{-1}, $E_C = 14.5$ kcal mol^{-1}.

Introduction

In the previous paper[1] we presented a detailed NMR study of the interconversion kinetics between the various isomers of fluorobullvalene (and other substituted bullvalenes) in solution. From the NMR line shapes of the ^{19}F and ^{13}C resonances the relative concentrations and the exchange rate of the various isomers were determined and used to derive thermodynamic and kinetic parameters for the system. In the present paper we extend this research to solid fluorobullvalene. Unlike in solution where all four possible isomers are present in equilibrium, in the solid state this compound crystallizes entirely as the single isomer 4 (with the fluorine bound to the bridgehead carbon), which is also the dominant species in solution.[1,2] Since this isomer has C_3 symmetry one would expect the molecules in the solid to undergo 3-fold jumps about their symmetry axes, a process which does not perturb the crystal order. On the other hand, Cope rearrangement seems less likely, since the bond shift reaction involves other isomeric species besides isomer 4, which are not stable in the crystalline state. We describe below 1D and 2D carbon-13 magic angle spinning (MAS) experiments on solid fluorobullvalene, which show that on the time scale of milliseconds the molecules indeed undergo 3-fold jumps, but that on a much longer time scale (of the order of seconds) they also undergo Cope rearrangement. The process involves isomers 1 and 3, as transient intermediates. Before describing these measurements we briefly report on the X-ray structure of fluorobullvalene.

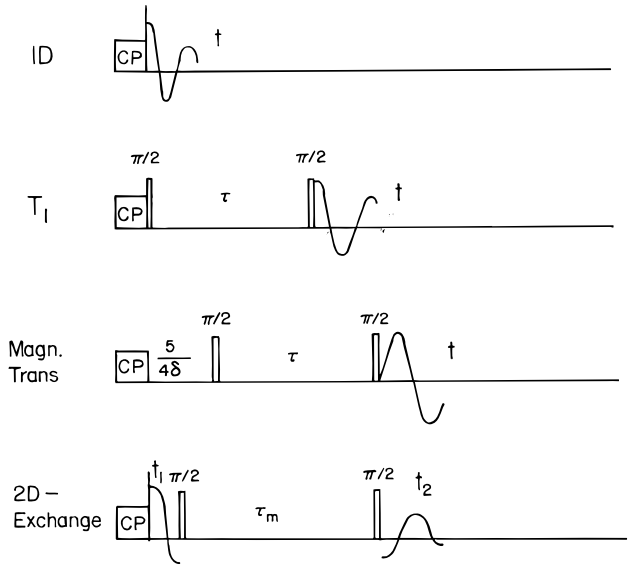

Figure 1. The pulse sequences used for the various solid state experiments. From top to bottom: cross polarization (CP) 1D MAS; inversion recovery T_1 experiment; magnetization transfer; rotor synchronized MAS 2D exchange.

Experimental Section

A. X-Ray Measurements. The X-ray measurements were made on a colorless prismatic crystal of dimensions, 0.15 × 0.20 × 0.35 mm, using an Enraf Nonius CAD4 circle diffractometer with a graphite monochromator (*MO-K*$_\alpha$, λ = 0.7107Å) and the ω-2θ scanning

[†] Univerität Stuttgart.
[‡] Max-Planck Institut für Medizinische Forschung.
[§] The Weizmann Institute of Science.
[⊗] Abstract published in *Advance ACS Abstracts,* August 1, 1996.

(1) Poupko, R.; Zimmermann, H.; Müller, K.; Luz, Z. *J. Am. Chem. Soc.* **1996**, *118*, 7995.
(2) Oth, J. F. M.; Merényi, R.; Röttele, H.; Schröder, G. *Tetrahedron Lett.* **1968**, *36*, 3941.

S0002-7863(95)04005-4 CCC: $12.00

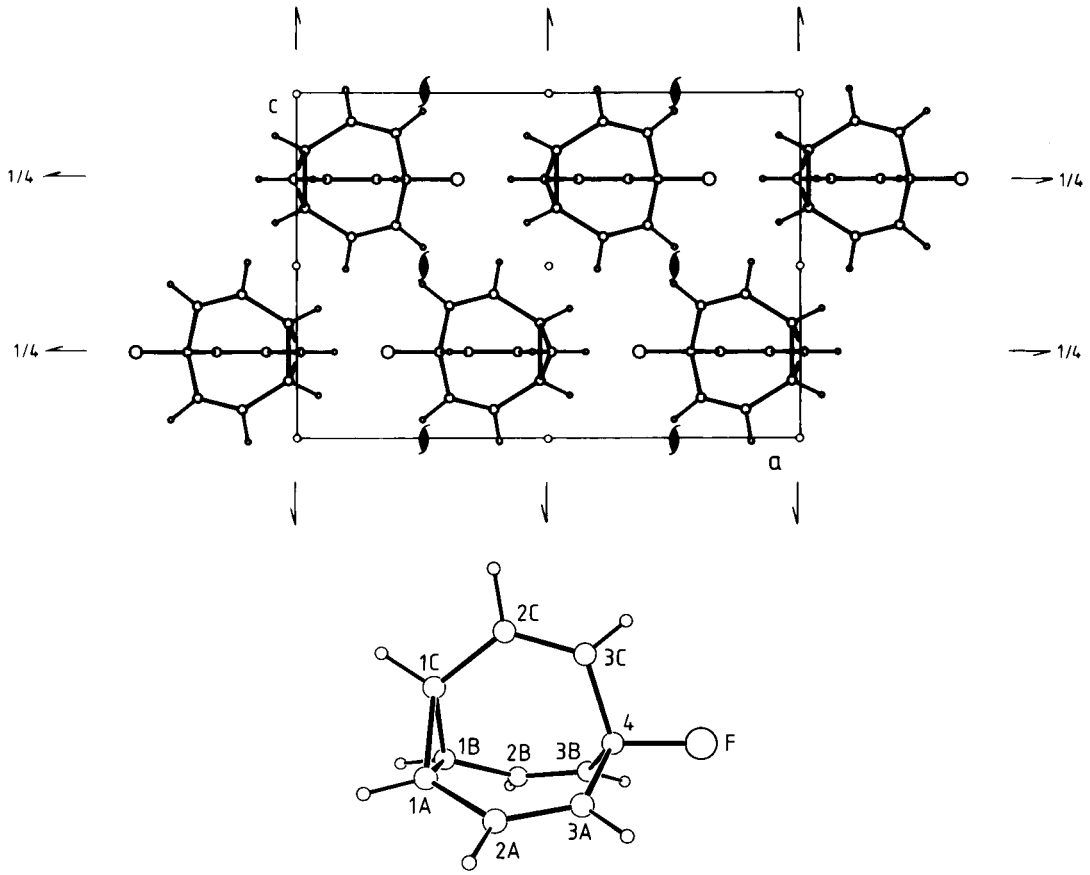

Figure 2. Top: Projection of the crystal structure of fluorobullvalene down the *b*-axis. The crystal is orthorhombic (space group *Pnam*) with four magnetically equivalent molecules per unit cell. Bottom: Perspective view of the fluorobullvalene molecule and the numbering system used.

technique. The structure was solved by direct methods (SIR)[3] and refined by matrix least squares, minimizing $\sum\omega\Delta F^2$ with the weight scheme $\omega = [\sigma(F)^2 + (0.03F_0)^2]^{-1}$. Isotropic (for H atoms) and anisotropic (for non-hydrogen atoms) displacement parameters were used until convergence was reached at $R/R_\omega = 0.043/0.051$. A total of 783 reflections were collected up to sin $\theta/\lambda = 0.62$ Å^{-1} of which 538 satisfied the criterion $I \geq 3.0\sigma(I)$.

B. NMR Measurements. The carbon-13 MAS spectra were recorded on Bruker CXP300 and MSL300 spectrometers at 75.46 MHz (7.05 T). Four types of experiments were performed (see Figure 1): (i) regular 1D MAS using cross polarization[4] (CP) ($\pi/2$ pulse width 4.5 μs, contact time 5 ms); (ii) T_1 inversion recovery measurements, where the π-flip was produced by CP followed in quadrature by a $\pi/2$ pulse;[5] and (iii) magnetization transfer spectra were obtained by the sequence shown in the third trace of Figure 1,[6] where τ is a variable mixing time and δ is the chemical shift (in Hz) between the peaks undergoing magnetization transfer. The carrier frequency is set halfway between these peaks and the evolution time, $1.25/\delta$, is adjusted so that at its end the two magnetizations are at antiphase to each other. To ensure that the succeeding $\pi/2$ pulse occurs at a rotation echo the spinning frequency ν_R was also synchronized with the evolution time.[6] (iv) Rotor synchronized 2D exchange MAS spectra[7] were obtained by the sequence shown in the bottom trace of Figure 1, with an eight step phase cycle as described in ref 8. Chemical shifts are given with respect to TMS. The spectrometer was calibrated using an adamantane sample taking $\delta(CH_2) = 38.56$ ppm and $\delta(CH) = 29.5$ ppm.

(3) Burla, M. C.; Camalli, M.; Cascarano, G.; Giacovazzo, C.; Polidori, G.; Spagna, R.; Viterbo, D. *J. Appl. Cryst.* **1989**, *22*, 389.
(4) Pines, A.; Gibby, M. G.; Waugh, J. S. *J. Chem. Phys.* **1973**, *59*, 569.
(5) Torchia, D. A. *J. Mag. Reson.* **1978**, *30*, 613.
(6) Szeverenyi, N. M.; Bax, A.; Maciel, G. E. *J. Am. Chem. Soc.* **1983**, *105*, 2579.
(7) Hagemeyer, A.; Schmidt-Rohr, K.; Spiess, H. W. *Adv. Magn. Reson.* **1989**, *13*, 85.
(8) Titman, J. J.; Luz, Z.; Spiess, H. W. *J. Am. Chem. Soc.* **1992**, *114*, 3756.

The Crystal Structure of Fluorobullvalene

Fluorobullvalene crystallizes entirely as isomer 4. The crystals are orthorhombic and belong to the space group *Pnam* (no. 62 in the International Table of X-ray Crystallography): $a = 13.411(3)$ Å, $b = 6.101(1)$ Å, $c = 9.191(3)$ Å. There are four, symmetry related, molecules per unit cell, two pairs related to each other by a center of symmetry, while each pair is related by a (screw) C_2 axis. A projection of the crystal structure onto the *ac* plane is shown in Figure 2. The molecules lie on mirror planes parallel to *ab* at $z = 1/4, 3/4$, and therefore in the crystal they have exact C_s symmetry (but very nearly C_{3v} symmetry with the angle between the equivalent wings being 118.8° and 120.6° between the nonequivalent wings). A perspective view of the molecule is shown in the bottom of Figure 2, which also includes the numbering system used in the present work. The mirror plane in the molecule includes the fluorine, carbon 4, and the atoms on wing *C* (1*C*, 2*C*, and 3*C*), and it bisects the angle between wings *A* and *B* (A^i). Some crystallographic data are summarized in Table 1. The complete data and the parameters of the structure refinement have been deposited with the Cambridge Crystallographic Data Center, 12 Union Road, Cambridge CB2 1EZ, United Kingdom. In these files wing *B* is labeled as A^i.

MAS Spectra in the Solid State

A. The Carbon-13 Chemical Shift Tensors and Longitudinal Relaxation. In Figure 3 are shown carbon-13 MAS spectra of fluorobullvalene at 15 °C for different spinning rates. Comparison with the low temperature solution spectrum[1] shows it to be consistent with that of isomer 4, in agreement with the X-ray results. It may be noticed that while carbons 1 exhibit a

Table 1. Some Crystallographic Parameters for the Non-Hydrogen Atoms of Fluorobullvalene[a]

A. Atomic Coordinates and Equivalent Isotropic Displacement Parameters

carbon/fluorine	*x*	*y*	*z*	$U_e(10^4/Å^2)$
4	0.2831(2)	0.0168(5)	0.2500	511(6)
3B	0.3029(1)	0.1496(3)	0.1165(2)	550(4)
2B	0.3912(1)	0.2256(3)	0.0831(2)	570(4)
1B	0.4833(1)	0.1968(3)	0.1666(2)	597(5)
3C	0.3409(2)	−0.1925(4)	0.2500	575(7)
2C	0.4392(2)	−0.1987(4)	0.2500	637(7)
1C	0.5057(2)	−0.0123(5)	0.2500	626(7)
F	0.1805(1)	−0.0390(3)	0.2500	816(5)

B. Bond Distances (in Å)

4-3B	1.494(2)	2B-1B	1.466(3)
4-3C	1.494(4)	1B-1C	1.518(3)
4-F	1.417(3)	3C-2C	1.319(4)
		1A-1B	1.553(3)

C. Bond Angles (in deg)

3B-4-3A	110.4(2)	2B-1B-1A	121.6(2)
3B-4-3C	111.8(1)	2B-1B-1C	122.1(2)
3B-4-F	107.6(1)	1A-1B-1C	59.7(1)
3C-4-F	107.4(2)	4-3C-2C	122.9(2)
4-3B-2B	123.1(2)	3C-2C-1C	126.4(3)
3B-2B-1B	126.7(2)	1B-1C-2C	122.7(2)
		1B-1C-1A	60.6(2)

[a] $U_{eq} = (1/3)\sum\sum U_{ij}\mathbf{a}_i\cdot\mathbf{a}_j a^*_j a^*_j$.

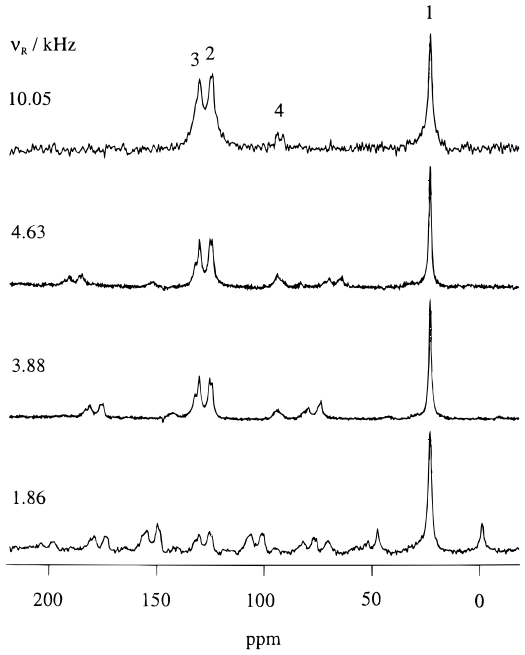

Figure 3. Carbon-13 MAS spectra of fluorobullvalene at 15 °C, at different spinning rates as indicated. The number of scans was 30 with recycle time of 7.5 min.

relatively sharp singlet the other peaks have some structure. At high spinning rates the signal of carbon 4 is an unequal doublet with a splitting of 160 Hz. This splitting is attributed to the scalar coupling with the fluorine nucleus, as it is identical to that found for $J_{^{19}F-^{13}C(4)}$ in solution.[1] The unequal intensity of the doublet components is due to the combined effects of the direct $^{19}F-^{13}C(4)$ dipolar interaction and the anisotropic chemical shift tensor of carbon 4 and will be further discussed in section C. The splittings observed in the olefinic carbon peaks 2 and 3 are too big to be due to spin−spin coupling with fluorine and are most likely due to chemical shift inequivalence of

Table 2. Carbon-13 Chemical Shift Tensors in Fluorobullvalene and Bullvalene[a,b]

	fluorobullvalene				bullvalene[c]			
	δ_{iso}	δ_{xx}	δ_{yy}	δ_{zz}	δ_{iso}	δ_{xx}	δ_{yy}	δ_{zz}
1	22.0	38	0	−38	22	35	−7	−28
2	125.5	86	0	−86	128	95	0	−95
3	131.0	86	0	−86	128	95	0	−95
4	92.0	30	30	−60	31			

[a] The isotropic chemical shifts are in ppm relative to TMS. Estimated accuracy ±0.2 ppm. [b] The principal values of the anisotropic tensors are in ppm relative to the corresponding δ_{iso}, so that $\delta_{xx} + \delta_{yy} + \delta_{zz} = 0$. Estimated accuracy ±5 ppm. [c] From ref 10.

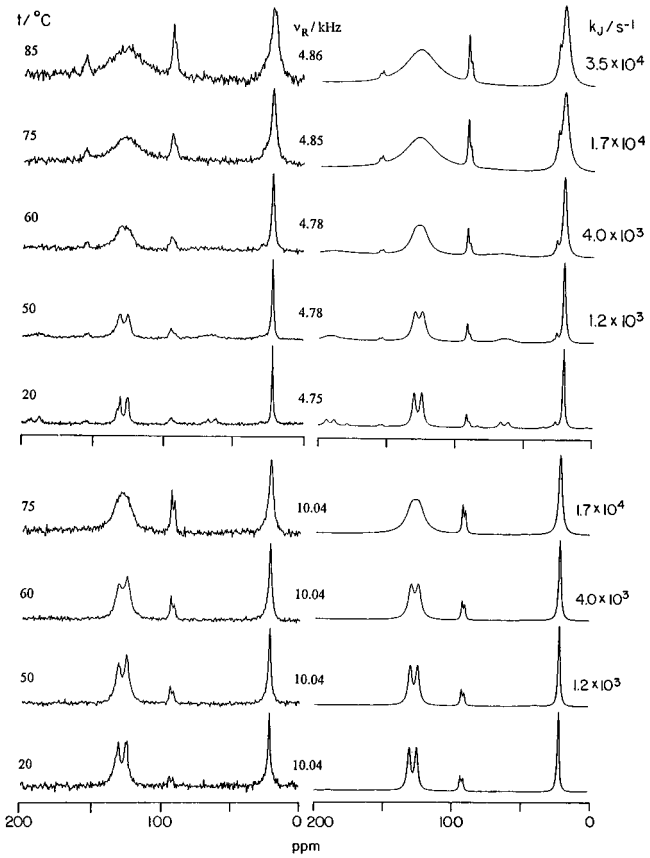

Figure 4. Left: Carbon-13 MAS spectra of fluorobullvalene at as function of temperature as indicated in the figure. The number of scans varied from 40 to 100 using a recycle time of 7.5 min. The line broadening parameters (LB) used in the Fourier transformation ranged from 0 (in the room temperature spectra) to 20 Hz (in the high temperature spectra). Right: Simulated spectra calculated for the experimental ν_R's and the indicated rates, k_J, for the 3-fold jumps. The magnetic and geometrical parameters used are explained in the text. The top five spectra are for $\nu_R \simeq 4.8$ kHz. The bottom four are for $\nu_R = 10.04$ kHz.

corresponding carbons in wing *C* and wings *A* and *B*. At low spinning frequencies, spinning side bands are observed for essentially all carbons in the spectrum. Using the Herzfeld−Berger theory[9] we have used these side bands to calculate the anisotropic chemical shift tensors of the various carbons. These are summarized in Table 2. For comparison, the values of unsubstituted bullvalene[10] are also included.

For the subsequent discussion it is necessary to have at least a good idea about the ^{13}C T_1's and their temperature dependence. These were measured as shown in the second trace of Figure 1

(9) Herzfeld, J.; Berger, A. E. *J. Chem. Phys.* **1980**, *73*, 6021.

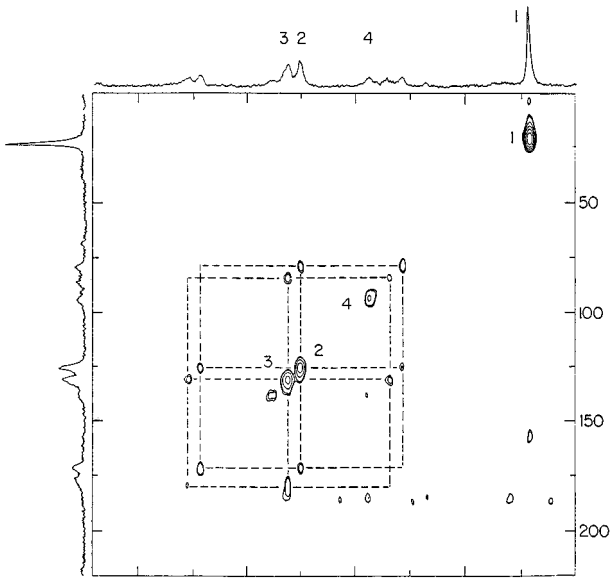

Figure 5. A carbon-13 rotor synchronized MAS 2D exchange spectrum of fluorobullvalene, recorded at 30 °C with a contact time of 5 ms, a mixing time $\tau_m = 20$ ms, and a rotor frequency of $\nu_R = 3.5$ kHz. Seventy-two t_1 increments of 50 μs were recorded, with a four-steps phase cycle for each of the regular and time reversed experiments (total of eight scans for each t_1). The dwell time was 25 μs, resulting in a sweep width of 20 kHz in both dimensions. The recycle time was 10 min, and the total measuring time was four days. Seven contours are plotted at powers of two intervals.

with sufficiently long recycle times. Measurements were made at 22 and 50 °C, yielding average T_1 values of respectively 52 and 11 min.

B. Line Broadening and the 2D Exchange Spectrum. In Figure 4 are shown temperature dependent MAS spectra of fluorobullvalene recorded at about 4.8 and 10.04 kHz. There is a clear selective line broadening. The peaks due to the olefinic carbons 2 and 3 broaden most, that of carbon 1 broadens less, while the peaks of carbon 4 does not broaden at all. In fact they appear to narrow upon heating with a concomitant improvement in resolution of the doublet structure. The extent of broadening also depends on the spinning rate, being larger for slower spinning. This behavior indicates the occurrence of a dynamic process, involving molecular reorientation and/or bond shift rearrangement. To preserve the crystal order the process must be such that whatever permutation of nuclei takes place, it should end up with the molecules in their original orientations in the crystal. Two exchange mechanisms that fulfill this requirement come to mind: (i) 3-fold jumps about the molecular pseudo C_3 axis and (ii) a sequence of Cope rearrangement involving transient isomeric species that, however, end up with the original ground state isomer 4. While the 3-fold jump process is easy to visualize, the rearrangement process is less obvious. We will discuss it in more detail in the last section of the paper. Qualitatively in the slow exchange regime (at the spinning rates used in our experiments) both processes have similar effects on the MAS spectrum. They result in broadening of peaks 1, 2, and 3 but do not affect the width of peak 4. In the intermediate and fast exchange regime the two mechanisms result in different spectral line shapes. However, since the compound melts at 97 °C we could only acquire slow exchange spectra, where they are not very sensitive to the exact mechanism of the dynamic process. A distinction between the two possibilities can, however, be made by MAS rotor synchronized 2D exchange spectroscopy.[7,8] This method leads to completely different patterns for the two mechanisms. While the 3-fold jumps process results only in auto cross peaks linking the main and side bands of the same type of carbons, the Cope rearrangement should, in addition, yield hetero cross peaks linking diagonal peaks of different carbons.[10] For both mechanisms the signal of carbon 4 should have no cross peaks at all.

In Figure 5 is shown a MAS rotor synchronized 2D exchange spectrum of fluorobullvalene, obtained at 30 °C with a mixing time of 20 ms. The spectrum clearly shows auto cross peaks of the two olefinic carbons 2 and 3 but conspicuously no hetero cross peaks with any of the other signals. We thus conclude that the line broadening observed in the 1D spectra of Figure 4 is due to 3-fold jumps. The lack of auto cross peak for carbon 1 in Figure 5 reflects the relative smallness of the chemical shift anisotropy of this carbon (cf. Table 2).

C. The Rate Constants for the 3-Fold Jump Process. Now, that the process responsible for the line broadening is known we can proceed to determine its rate at the various temperatures by comparing the experimental MAS spectra with appropriate simulations. For the 3-fold jump process the broadening is entirely due to the anisotropy of the chemical shift tensors and should therefore be sensitive to the spinning rate. This is indeed the case as may be seen by comparing the spectra in Figures 4 and 5. To simulate these spectra we apply the theory of Schmidt and Vega for dynamic line shapes under magic angle spinning conditions.[11,12] According to this theory the time domain signal is given by

$$S(t) = \sum_{i,j} \sum_{n=-\infty}^{\infty} \langle in| \exp(-iH_F t)|j0\rangle e^{in2\pi\nu_R t} P_j \qquad (1)$$

where the indices i,j label the exchanging sites and the n's are integers that label the spinning side bands. In practice they range over the limited number of observable side bands, and the sum over them is truncated by checking the convergence of the calculated spectra. H_F is the so called Floquet Hamiltonian with elements

$$\langle in|H_F|jn'\rangle = (\omega^i_{n-n'} + n2\pi\nu_R\delta(n-n'))\delta(i-j) + ik_{ij}\delta(n-n') - \frac{1}{T_2}\delta(i-j)\delta(n-n') \qquad (2)$$

where k_{ij} are the elements of the exchange matrix, K, describing the dynamic process, $\omega^i_{n-n'}$ are the Fourier components of the expansion of the anisotropic interaction in the basis of the spinning frequency and $\delta(l-k)$ are delta functions. For an anisotropic chemical shift tensor they are

$$\omega^i_0 = \omega_L\delta^i_{iso}$$

$$\omega^i_1 = \frac{1}{2}\omega_L(C^i_1 - iS^i_1)\exp(i\gamma) = (\omega^i_{-1})^* \qquad (3)$$

$$\omega^i_2 = \frac{1}{2}\omega_L(C^i_2 - iS^i_2)\exp(i2\gamma) = (\omega^i_{-2})^*$$

$$\omega^i_k = 0 \quad \text{for } |k| > 2$$

where ω_L is the rotating frame frequency and

(10) Titman, J. J.; Luz, Z.; Spiess, H. W. *J. Am. Chem. Soc*. **1992**, *114*, 3765.
(11) Schmidt, A.; Vega, S. *J. Chem. Phys*. **1987**, *87*, 6895.
(12) Luz, Z.; Poupko, R.; Alexander, S. *J. Chem. Phys*. **1993**, *99*, 7544.

$$C_1^i = \frac{\sqrt{2}}{3}\left\{-\frac{3}{2}\delta_{33}^i \sin 2\beta - \left[\frac{1}{2}(\delta_{22}^i - \delta_{11}^i)\cos 2\alpha - \delta_{12}^i \sin 2\alpha\right]\sin 2\beta + 2\,[\delta_{13}^i \cos\alpha + \delta_{23}^i \sin\alpha]\cos 2\beta\right\} \quad (4a)$$

$$S_1^i = \frac{2\sqrt{2}}{3}\left\{\left[\frac{1}{2}(\delta_{22}^i - \delta_{11}^i)\sin 2\alpha + \delta_{12}^i \cos 2\alpha\right]\sin\beta - [\delta_{13}^i \sin\alpha - \delta_{23}^i \cos\alpha]\cos\beta\right\} \quad (4b)$$

$$C_2^i = \frac{1}{3}\left\{\frac{3}{2}\delta_{33}^i \sin^2\beta - \frac{1}{2}\left[\frac{1}{2}(\delta_{22}^i - \delta_{11}^i)\cos 2\alpha - \delta_{12}^i \sin 2\alpha\right]\times(\cos 2\beta + 3) - (\delta_{13}^i \cos\alpha + \delta_{23}^i \sin\alpha)\sin 2\beta\right\} \quad (4c)$$

$$S_2^i = \frac{2}{3}\left\{\left[\frac{1}{2}(\delta_{22}^i - \delta_{11}^i)\sin 2\alpha + \delta_{12}^i \cos 2\alpha\right]\cos\beta + [\delta_{13}^i \sin\alpha - \delta_{23}^i \cos\alpha]\sin\beta\right\} \quad (4d)$$

The $\delta_{\mu\nu}^i$ in eqs 4 are the components of the chemical shift tensor of the ith atom in the molecular frame with $\sum_{\mu=1}^{3}\delta_{\mu\mu} = 0$ and α, β, and γ are the (Euler) angles that transform this tensor to the rotor frame. For a powder sample an isotropic integration over these angles must be performed.

For the 3-fold jumps there is no exchange between different types of atoms. Consequently for each triad of atoms *iA*, *iB*, and *iC*, $i = 1, 2, 3$ and we have the same exchange matrix[13,14]

$$K_J = k_J\begin{pmatrix} -1 & \frac{1}{2} & \frac{1}{2} \\ \frac{1}{2} & -1 & \frac{1}{2} \\ \frac{1}{2} & \frac{1}{2} & -1 \end{pmatrix} \quad (5)$$

where k_J is the rate constant of the reaction. The spectrum of atom 4 is not affected by the 3-fold jump process and is therefore not included in the calculations.

The Herzfeld−Berger analysis[9] only provides principal values for the anisotropic chemical shift tensors δ(PAS) (δ_{xx}, δ_{yy}, δ_{zz}) but not their principal directions in the molecular frame. For the application of eqs 4 we therefore need to make assumptions regarding the orientations of the various tensors in the molecule. For the olefinic carbons we follow the procedure used earlier[10,12] for the case of bullvalene. We take $\delta_{yy}^{i\alpha}$ to be parallel to the double bond of atom i ($i = 2$ or 3) in the α wing ($\alpha = A$, B, or C), $\delta_{zz}^{i\alpha}$ to be perpendicular to the plane of the α wing, and $\delta_{xx}^{i\alpha}$ in the α plane perpendicular to both $\delta_{yy}^{i\alpha}$ and $\delta_{zz}^{i\alpha}$. We also assumed that the molecules in the solid have C_3 symmetry, with all the angles between the double bond and the C_3 axis equal, $\theta = 14.2°$. The elements, $\delta_{\nu\mu}^{i\alpha}$, of the anisotropic chemical shift tensors of the olefinic carbons in the molecular frame (MF) are then given by

$$\delta^{i\alpha}(MF) = R(\theta,\phi^\alpha)\delta^{i\alpha}(PAS)R^{-1}(\theta,\phi^\alpha) \quad (6)$$

where

$$\delta^{i\alpha}(PAS) = \begin{pmatrix} \delta_{xx}^{i\alpha} & 0 & 0 \\ 0 & \delta_{zz}^{i\alpha} & 0 \\ 0 & 0 & \delta_{yy}^{i\alpha} \end{pmatrix} \quad (7)$$

and

$$R(\theta,\phi^\alpha) = \begin{pmatrix} \cos\theta\cos\phi^\alpha & \sin\phi^\alpha & -\sin\theta\cos\phi^\alpha \\ -\cos\theta\sin\phi^\alpha & \cos\phi^\alpha & \sin\theta\sin\phi^\alpha \\ \sin\theta & 0 & \cos\theta \end{pmatrix} \quad (8)$$

with $\phi^\alpha = 0$, 120, and 240 for the wings *A*, *B*, and *C*, respectively.

In order to get a feeling for the expected behavior of the dynamic MAS spectrum we have computed such spectra for a single type of olefinic carbon, for the two spinning frequencies, $\nu_R = 4.75$ and 10.0 kHz. As function of the jumps rate, the results showed an initial line broadening of the main peak and its side bands, followed by line narrowing and a modified (intensity-wise) spinning side bands pattern. The overall width of the spectrum (full width at half maximum intensity), which is essentially the width of the center band, is plotted in Figure 6 as function of k_J for both values of ν_R (curves a and b). It may be seen that at higher spinning rates the broadening is smaller, and the point of maximum broadening is shifted to higher values of k_J. To derive rate constants for the 3-fold jump process we fitted simulated spectra, which were calculated as a superposition of the two types of olefinic carbons, to the experimental results. The small (structure related) splitting of the lines was accounted for by an effective line width parameter of $1/T_2^\circ = 690\ s^{-1}$. Such simulated spectra, which include also the simulations of the signals due to carbons 1 and 4, to be described shortly, are shown in the right column of Figure 4 for the indicated values of k_J. The rate constants so derived are plotted in Figure 7 versus the reciprocal absolute temperature, yielding the Arrhenius equation

$$k_J(s^{-1}) = 6.0 \times 10^{17}\exp(-E_J/RT)$$

with $E_J = 21.7$ kcal mol^{-1}.

In principle the broadening of the signal due to the cyclopropane ring carbons (1A, 1B, and 1C) could also be used to derive k_J. However since the anisotropy of their chemical shift tensors is quite small, their signal undergoes much less broadening compared to the olefinic carbons which renders it less suitable for rate measurements. Also we have less knowledge about the orientations of their chemical shift tensors in the molecular frame. In solid cyclopropane the carbon-13 chemical shift tensor was determined by Zilm et al.[15] at low temperatures. They obtained, $\delta_{xx} = 26$ ppm, $\delta_{yy} = 6$ ppm, and $\delta_{zz} = -32$ ppm (relative to $\delta_{iso} = -4$ ppm) with δ_{zz} parallel to the molecular C_3 axis, δ_{xx} along the C_2 axis containing the carbon atom, and δ_{yy} in the molecular plane, perpendicular to both δ_{xx} and δ_{zz}. Comparing with the results for carbons 1 in fluorobullvalene (Table 2) and considering the local symmetry of these atoms, we can safely conclude that the principal directions associated with $\delta_{yy}^{1\alpha}$ is perpendicular to the plane of the α wing and that those associated with $\delta_{xx}^{1\alpha}$ and $\delta_{zz}^{1\alpha}$ lie in the plane of the α wing, but their orientations within this plane is not known. We therefore reverse the procedure and use the experimental broadening of the carbons 1 signals together with the known jump rates to determine the angle θ', between the principal direction associated with δ_{zz}^1 and the molecular C_3 axis. Calculated dynamic line width of the carbon 1 signal at $\nu_R = 4.75$ kHz as function of k_J for two θ' values, 0° and 45°, are shown in Figure 6 (curves d and c). It may be seen that the

(13) Schlick, S.; Luz, Z.; Poupko, R.; Zimmermann, H. *J. Am. Chem. Soc.* **1992**, *114*, 4315.
(14) Müller, A.; Haeberlen, U.; Zimmermann, H.; Poupko, R.; Luz, Z. *Mol. Phys.* **1994**, *81*, 1239.
(15) Zilm, K. W.; Allred, E. L.; Beeler, A. J.; Chou, T. C.; Grant, D. M.; Michl, J. *J. Am. Chem. Soc.* **1981**, *103*, 2119.

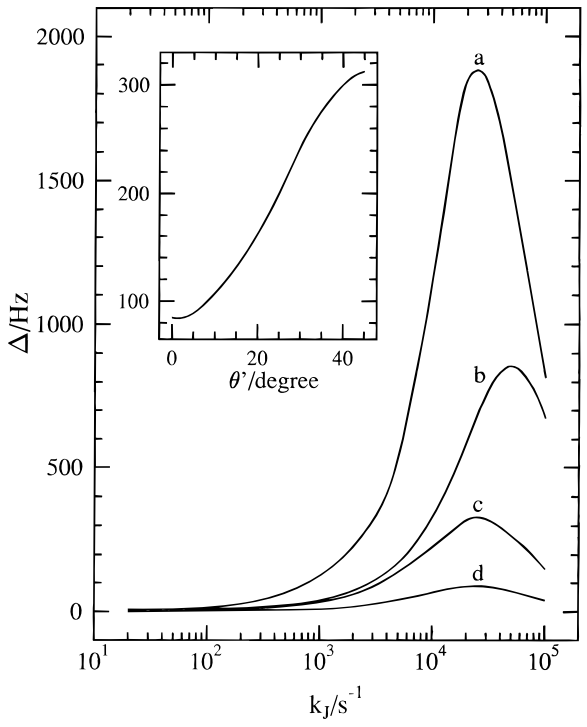

Figure 6. Calculated overall width (full width at half maximum intensity) of the MAS spectrum of single types of fluorobullvalene carbons as function of the rate constant, k_J, of the 3-fold jump process. Curves a and b are for the olefinic carbons (2, 3) at, respectively, ν_R = 4.75 and 10.0 kHz, with θ = 14.2°. Curves c and d are for the cyclopropane ring carbons (1) at ν_R = 4.75 kHz with θ' = 45° and 0°, respectively. The magnetic parameters were taken from Table 2. The insert gives the line width of carbons 1 at ν_R = 4.75 kHz and k_J = 3.5 × 10^4 s^{-1} as function of θ'.

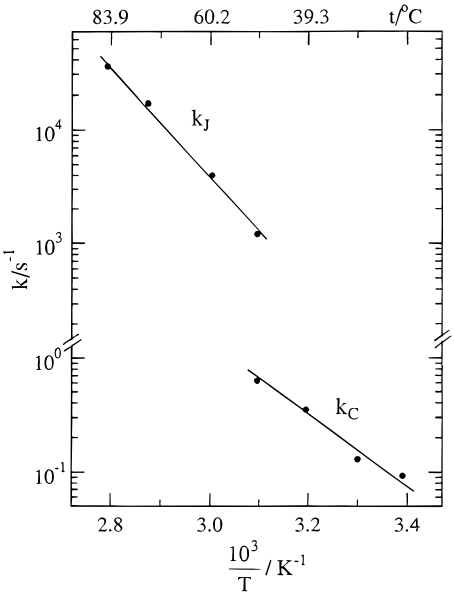

Figure 7. Arrhenius plots for the rate constants of the 3-fold jumps, k_J, and for the Cope rearrangement, k_C, in solid fluorobullvalene.

width is quite sensitive to θ'. This is shown more clearly in the insert to the figure, where the overall line width, for ν_R = 4.75 kHz and $k_J = 3.5 \times 10^4$ s^{-1}, is plotted as function of θ' in the range 0° to 45°. Since δ^1_{xx} and δ^1_{zz} have the same magnitude differing only in sign, the θ' dependence reverses on going from 45° to 90°. For these calculations we used the δ^1 tensor from Table 2 with eqs 1−8 as above. The only change is in eq 10, where in order to conform with the assigned directions of the principal components should now read

$$\delta^i(PAS) = \begin{pmatrix} \delta^i_{xx} & & \\ & \delta^i_{yy} & \\ & & \delta^i_{zz} \end{pmatrix} \qquad (9)$$

Referring to the experimental spectrum for ν_R = 4.87 kHz at 85 °C (Figure 4), for which k_J was found to be 3.5 × 10^4 s^{-1}, and the insert in Figure 6, we note that the observed line width of carbons 1 (∼420 Hz) corresponds, approximately, to the largest possible broadening (330 Hz plus the natural line width). This means that θ' is approximately 45°. Using this value and the k_J results from the olefinic carbons we computed the dynamic MAS spectra of carbons 1 shown in the right column of Figure 4.

To complete the simulation we also added the exchange invariant signal of carbon 4. The uneven scalar splitting of this carbon was taken into account by calculating two sets of Herzfeld−Berger spinning side bands centered, respectively, at $\nu_L\delta^4_{iso} \mp 1/2J_{^{19}F-^{13}C(4)}$ with effective axially symmetric chemical shift tensors, $\nu_{||} = \nu_L\delta^4_{zz} \pm 1/2D$ and $\nu_\perp = \nu_L\delta^4_{yy} \mp 1/4D$ where $D = (2h\gamma_F\gamma_C)/r^3$ = 19.98 kHz is the $^{19}F-^{13}C(4)$ dipole−dipole interaction and r is the F−C(4) bond length (1.417 Å). Here we have assumed that the unique direction, z, of the carbon 4 chemical shift tensor is collinear with the F−C(4) bond direction, as implied by the symmetry of the molecule. From the fact that the high field component of the center band doublet in the spectrum of carbon 4 is smaller than the low field one, it follows (as it also does from the simulation) that the sign of $J_{^{19}F-^{13}C(4)}$ is negative, as usually found for $^1J_{^{19}F-^{13}C}$.[16] The calculated relative intensities of the doublet components fits reasonably well the experimental results. It should be noted that these relative intensities are sensitive to the $|\nu_L\delta_{zz}|/|1/2D|$ ratio, particularly when it is close to unity, as in our case. For a more complete simulation also a possible contribution from the anisotropic $^1J_{^{19}F-^{13}C(4)}$ interaction must be considered.

Finally, to account for the nonstoichiometric intensity of peak 4 (due to its lower CP efficiency) its integrated intensity (the first point of its time domain spectrum) was normalized to 0.7 (rather than 1) compared to 3 for all other carbons. This value was chosen to fit the experimental spectra at 20 °C and was retained for all other temperatures. The spectra were calculated with exchange invariant $1/T_2$'s that took into account the inhomogeneous broadening due to the crystallographic inequivalence of the carbons on wing C and those of wings A and B. These were, 380 s^{-1} for carbon 1 and 690 s^{-1} for carbons 2 and 3. For carbon 4 a value of 345 s^{-1} was taken. Calculations were made with n = 4 and 6 (in eq 1) for the ν_R = 10.04 and 4.8 kHz spectra, respectively (corresponding to 9 and 13 spinning side bands) and summed over 538 sampling points (α, β, and γ) for each spectrum using the Conroy−Wolfsberg algorithm.[17]

D. Magnetization Transfer and 2D Exchange Spectra on the Time Scale of Seconds. We have seen that at room temperature and above, fluorobullvalene undergoes 3-fold jumps in the submillisecond time regime, but no sign of chemical exchange (Cope rearrangement) was detected. To check

(16) Wehrli, F. W.; Marchand, A. P.; Wehrli, S. Interpretation of Carbon-13 NMR Spectra, 2nd ed.; John Wiley and Sons: Chichester, 1988; p 92.

(17) Conroy, H. *J. Chem. Phys.* **1967**, *47*, 5307. Cheng, V. B.; Suzukawa, H. H.; Wolfsberg, M. *J. Chem. Phys.* **1973**, *59*, 3992. Suzukawa, H. H.; Thompson, D. L.; Cheng, V. B.; Wolfsberg, M. *J. Chem. Phys.* **1973**, *59*, 4000.

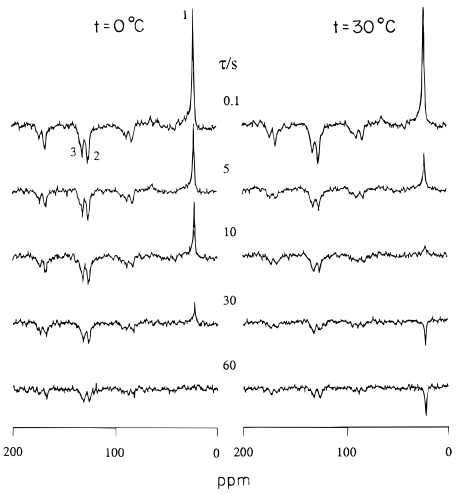

Figure 8. Carbon-13 magnetization transfer spectra of fluorobullvalene as function of the mixing time, τ, at 0 °C (left) and 30 °C (right). The carrier frequency was set halfway between signal 1 and the midpoint frequency of the olefinic carbons 2, 3. The spinning frequency was 3.2 kHz, the evolution period $5/4\delta = 313$ μs, the recycle time 10 min and the number of scans 6. The spectrum intensity in each column is normalized with respect to the first trace at $\tau = 0.1$ s.

whether such a process does take place on a longer time scale, of the order of seconds, we have performed magnetization transfer experiments of the type described in the third trace in Figure 1.[6] Such experiments are feasible since the carbon-13 T_1's are of the order of many minutes at low temperatures. Particularly sensitive to the Cope rearrangement is the magnetization transfer between carbon 1 and the olefinic carbons 2 and 3 and between carbons 1 and 4.

In Figure 8 are shown two series of magnetization transfer spectra for 0 and 30 °C. These experiments were done with the carrier rf frequency half way between the resonance frequency of carbon 1 and the midpoint of those due to the olefinic carbons 2 and 3. Very significant changes in the peak intensities as function of the mixing times are observed, with characteristic decay times of the order of 10 s at 0 °C and ~3 s at 30 °C. These values are much shorter than the measured T_1's at corresponding temperatures and must therefore reflect genuine magnetization transfer. The pronounced temperature dependence suggests that the spin exchange is due to Cope rearrangement rather than spin diffusion. A stronger proof for this conclusion is provided by the 2D exchange spectra described below. We have not carried out an exact quantitative analysis of the magnetization transfer experiments since the signals are expected to follow multiexponential decay curves whose interpretation requires very accurate (and therefore very long) measurements. However a rough estimate of the kinetic parameters could be obtained from the initial decay of the various signals. Such estimated values, which we identify with the Cope rearrangement rate constants, k_C, are plotted in Figure 7 (together with those for k_J), yielding an Arrhenius equation with a pre-exponential factor $A_C = 4.6 \times 10^9$ s^{-1} and an activation energy $E_C = 14.5$ kcal mol^{-1}.

A more direct proof for the occurrence of the Cope rearrangement in solid fluorobullvalene was obtained by rotor synchronized MAS 2D exchange experiments,[7,8] with mixing times in the seconds regime. Two such 2D exchange spectra are shown in Figure 9, for $\tau_m = 2$ s (left) and 20 s (right). The spectra clearly show, in addition to the auto cross peaks discussed before, also hetero cross peaks between different types of carbons that can only result from the Cope rearrangement process. Note that, here too, no cross peaks involving carbon 4 are observed. This selectivity further supports the ruling out of spin diffusion as a mechanism for the magnetization transfer.

E. The Mechanism of the Cope Rearrangement in Crystalline Fluorobullvalene. The question arises as to the mechanism of the Cope rearrangement in solid fluorobullvalene. Since it consists entirely of isomer 4, we must assume that the process leading to the hetero cross peaks in the 2D exchange spectra of Figure 9 involves a sequence of interconverting isomers ending up in a rearranged isomer 4. Carbon 4 must resume its original site in the crystal, but the other carbons may be permuted. Referring to the interconversion scheme of the preceding paper[1]

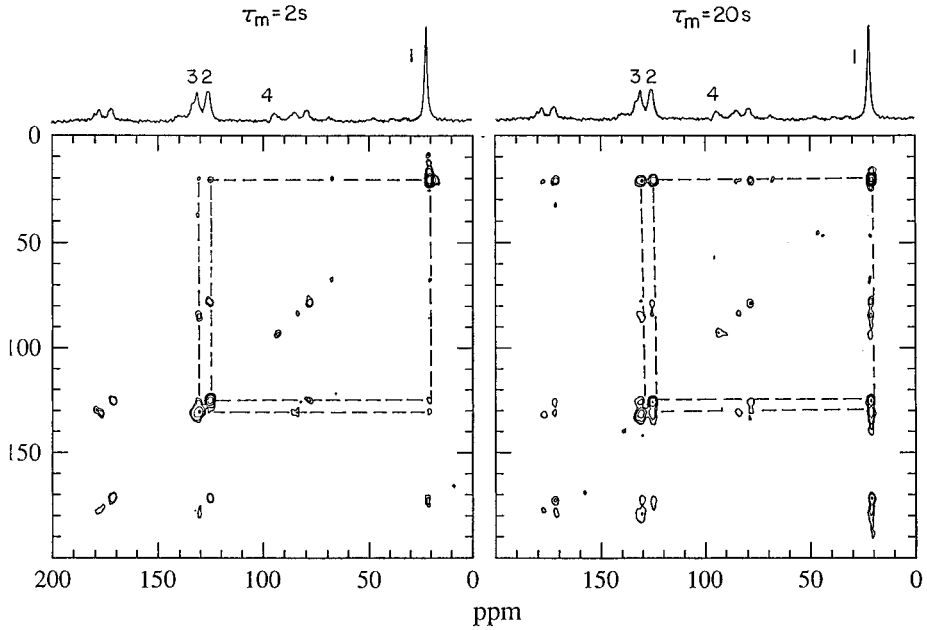

Figure 9. Carbon-13 rotor synchronized MAS 2D exchange spectra of fluorobullvalene recorded at 22 °C with $\nu_R = 3.5$ kHz and mixing times of $\tau_m = 2$ s (left) and $\tau_m = 20$ s (right). Other details are as in Figure 5. The dashed lines link hetero cross peaks of the center bands of peaks 1, 2, and 3.

only a limited number of cycles need be considered. These are

(i) $4 \rightarrow 1 \rightarrow 4$

(ii) $4 \rightarrow 1 \rightarrow 3 \rightarrow 1 \rightarrow 4$

(iii) $4 \rightarrow 1 \rightarrow 3 \rightarrow 2 \rightarrow 3 \rightarrow 1 \rightarrow 4$

(iv) $4 \rightarrow 1 \rightarrow 3 \rightarrow 2 \rightarrow 2 \rightarrow 3 \rightarrow 1 \rightarrow 4$

(v) $4 \rightarrow 1 \rightarrow 3 \rightarrow 2 \rightarrow 2 \rightarrow 2 \rightarrow 3 \rightarrow 1 \rightarrow 4$

Each of these cycles starts and ends with isomer 4 but involves different intermediates. The different cycles will in general lead to different permutations and therefore will correspond to different exchange matrices. Thus the 2D exchange spectra can in principle be used to identify the rearrangement mechanism that actually takes place in fluorobullvalene. In the following we analyze the various sequences indicated above. We start with sequence (i), where the original atom labeling is preserved

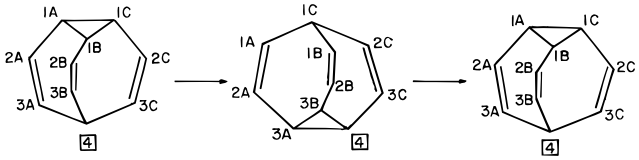

throughout the cycle and the substituted atom is enclosed in a square. To avoid repeated drawing of the bullvalene skeleton and to facilitate the analysis of the bond shift rearrangement we shall describe these sequences in the form of numerical diagrams, as shown below for the above sequences

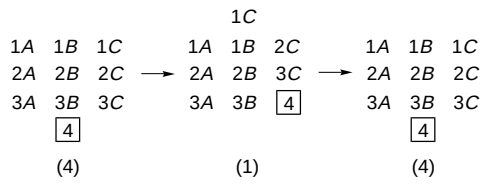

In these diagrams the columns represent the wings and the isolated atom corresponds to the bridgehead carbon. The two rows next to the bridgehead atom correspond to the olefinic carbons and the final row of atoms (opposite the bridgehead atom) to the aliphatic cyclopropane ring atoms. The Cope rearrangement is represented by the "pushing" up or down of the bridgehead atom and the three atoms of one of the wings. The bridgehead atom then becomes a cyclopropane ring atom and the corresponding original cyclopropane ring atom becomes the new bridgehead carbon. In the above sequence we chose to "push" carbon 4 and wing *C*, but the reaction could also proceed via wings *B* or *A*. The point to notice is, however, that in order for the intermediate isomer 1 to return to the ground state isomer 4, the same wing that was "pushed up" in the first step (wing *C* in the above scheme) must be "pushed down" in the second step. Consequently no permutation of atoms can occur by this mechanism. Thus, although this process most likely takes place in solid fluorobullvalene, it cannot be responsible for the dynamic effects observed in the experiments.

We next consider mechanism (ii), $4 \rightarrow 1 \rightarrow 3 \rightarrow 1 \rightarrow 4$, in which the ground state isomer transforms into isomer 1, which in turn transforms into isomer 3 and then back via 1 to 4

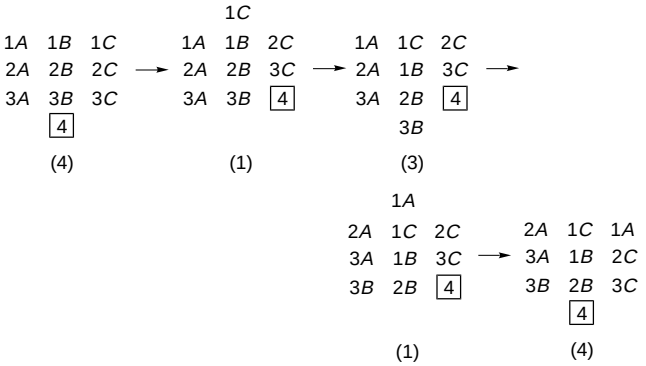

Here the first step is as in the previous mechanism, but it is followed by "pushing" down and up of, respectively, wings *B* and *A*, before wing *C* is pushed down again. Notice, however, that the "pushing down" of wing *B* in the $1 \rightarrow 3$ step corresponds to cleavage of the *s*-bond 3A-4 (i.e., a neighboring bond to the substituted wing), while the "pushing up" of wing *A* in the $3 \rightarrow 1$ step involves cleavage of the *s*-bond $1C-2C$ which is on the other side of the substituted wing. If the second step would involve "pushing up" of column *B*, the sequence would exactly revert itself, and no permutation of atoms would take place. We may assume that this will be the case in 50% of the exchanges.

By comparing the atom numbering in the final and initial isomers 4 the following overall exchange matrix is obtained

$$K_C^{1,3,1} = k_C^{1,3,1} \begin{pmatrix} -\frac{1}{3} & \frac{1}{3} & 0 & 0 \\ \frac{1}{3} & -\frac{2}{3} & \frac{1}{3} & 0 \\ 0 & \frac{1}{3} & -\frac{1}{3} & 0 \\ 0 & 0 & 0 & 0 \end{pmatrix}$$

where the rows and columns correspond sequentially to carbons 1, 2, 3, and 4 and the superscript 1,3,1 indicates the transient intermediates involved in this mechanism. The rows and columns in the exchange matrix correspond to the groups of three carbons 1, 2, and 3 and the single carbon 4. Exactly identical exchange matrices would be obtained if in the initial $4 \rightarrow 1$ step columns *A* or *B* would be pushed up. The rate constant $k_C^{1,3,1}$, corresponds to half of the occurrences of the 4-1-3-1-4 sequences since, as indicated above, in half of the cases no permutation occurs. Note that the process also brings about permutation of atoms of the same type (atom switching between wings) which has the effect of a reorientation. We need, however, not consider this effect here, since the much faster 3-fold jumps completely mask this effect in the 2D exchange spectrum.

The relative intensities of the signals in a 2D exchange spectra are given by[18,19]

$$S(\tau_m)_{ij} = [\exp(-K\tau_m)]_{ij} P_j = \left[\mathbf{1} - K\tau_m + \frac{1}{2}K^2\tau_m^2 - \frac{1}{6}K^3\tau_m^3 + \ldots\right]_{ij} P_j \quad (10)$$

From the exchange matrix, $K_C^{1,3,1}$, we thus predict the appearance of first order cross peaks (i.e., cross peaks that increase

(18) Ernst, R. R.; Bodenhausen, G.; Wokaun, A. Principles of nuclear magnetic resonance in one and two dimensions; Clarendon Press: Oxford, 1987; Chapter 9.

(19) Boeffel, C.; Luz, Z.; Poupko, R.; Zimmermann, H. *J. Magn. Reson.* **1989**, *85*, 329.

linearly with τ_m) between carbons 1 and 2 and between carbons 2 and 3, but only second order cross peaks (which increase as τ_m^2) between carbons 1 and 3. Inspection of the 2D spectra in Figure 9 shows that for $\tau_m = 20$ s (which corresponds to $k_C\,\tau_m \gg 1$) the various hetero cross peaks are equally strong, while for $\tau_m = 2$ s (where $k_C\,\tau_m \lesssim 1$) the 1, 3 cross peaks are significantly weaker than those for 1, 2 and 2, 3. We believe that this observation provides strong evidence for the occurrence of mechanism (ii) in solid fluorobullvalene. In principle one could study the evolution of the cross peak intensity with τ_m, but this would require prohibitively long measuring times. A schematic trajectory of mechanism (ii) is shown in Figure 10.

Considering the next sequence (iii), which involves in addition to isomers 1 and 3 also isomer 2 as an intermediate, we note that its interconversion from, and to, isomer 3 involves cleavage of the bond opposite (an *a* bond) the substituted wing. As discussed in connection with sequence (i), such a process does not lead to permutation of atoms and therefore the overall effect of mechanism (ii) on the NMR spectrum is the same as that of mechanism (ii).

Sequences (iv) and (v) on the other hand do lead to atom permutation. Proceeding as above the following exchange matrix is derived for mechanism (iv)

$$K_C^{1,3,2,2,3,1} = k_C^{1,3,2,2,3,1}\begin{pmatrix} -\frac{7}{12} & \frac{5}{12} & \frac{2}{12} & 0 \\ \frac{5}{12} & -\frac{7}{12} & \frac{2}{12} & 0 \\ \frac{2}{12} & \frac{2}{12} & -\frac{4}{12} & 0 \\ 0 & 0 & 0 & 0 \end{pmatrix}$$

while for (v)

$$K_C^{1,3,2,2,2,3,1} = k_C^{1,3,2,2,2,3,1}\begin{pmatrix} -\frac{8}{12} & \frac{7}{12} & \frac{1}{12} & 0 \\ \frac{7}{12} & -\frac{9}{12} & \frac{2}{12} & 0 \\ \frac{1}{12} & \frac{2}{12} & -\frac{3}{12} & 0 \\ 0 & 0 & 0 & 0 \end{pmatrix}$$

where, as before, the superscripts label the sequence of intermediates involved in the rearrangement. In principle high precision 2D exchange measurements over a wide range of τ_m value could tell whether these processes also occur. They must however be slower than mechanism (ii), since the latter is nested within these larger cycles.

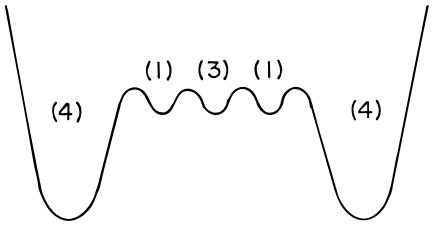

Figure 10. Schematic trajectory of the Cope rearrangement pathway in solid fluorobullvalene. The ground-state isomer 4 interconverts into itself via the transient intermediates isomers 1 and 3.

Summary and Discussion

Solid fluorobullvalene consists purely of isomer 4 as the ground state species. Due to the pseudo C_3 symmetry of these molecules they can readily undergo 3-fold jumps without introducing disorder in the crystal lattice. In fact this process takes place on the milisecond time scale at room temperature and much faster at higher temperatures. Unlike in the case of unsubstituted bullvalene,[13,14] fluorobullvalene cannot undergo a single Cope rearrangement step in the solid state, since such a process necessarily leads to a different isomer (1) which cannot be accommodated in the lattice. If it forms it can only be short lived, immediately reverting to the ground isomeric form (4). Such an event however will not lead to permutation of the carbon atoms in fluorobullvalene and will therefore not be detected by NMR. Experimentally, permutation between carbon atoms are observed in solid fluorobullvalene on the time scale of seconds (at room temperature), yielding characteristic 2D exchange spectra. These results indicate the occurrence of a more complicated sequence of rearrangements involving at least two isomers, 1 and 3, as transient intermediates and possibly also isomer 2. As these intermediates are very unstable in the crystal lattice the Cope rearrangement in fluorobullvalene is much slower than in unsubstituted bullvalene, where it is of the order of 10^4 s^{-1} (at room temperature).[13]

Acknowledgment. This research was supported by Grant No. 92-0094/5862 from the United States−Israel Binational Science Foundation (BSF), Jerusalem, Israel, and by the MINERVA Foundation, Munich/Germany. One of us (K.M.) thanks the Fonds der Chemischen Industrie for financial support.

Supporting Information Available: A listing of crystallographic data (3 pages). See any current masthead page for ordering information and Internet access instructions.

JA954005L